Cell Death and Differentiation (2011) 18, 259–270

www.nature.com/cdd

COP9 signalosome subunit 8 is required for postnatal hepatocyte survival and effective proliferation

D Lei[1,2], F Li[2,3], H Su[1,2], Z Tian[1], B Ye[3], N Wei[4] and X Wang*[,1,2]

Studies using lower organisms and cultured mammalian cells have revealed that the COP9 signalosome (CSN) has important roles in multiple cellular processes. Conditional gene targeting was recently used to study CSN function in murine T-cell development and activation. Using the Cre-loxP system, here we have achieved postnatal hepatocyte-restricted knockout of the *csn8* gene (HR-Csn8KO) in mice. The protein abundance of other seven CSN subunits was differentially downregulated by HR-Csn8KO and the deneddylation of all cullins examined was significantly impaired. Moreover, HR-Csn8KO-induced massive hepatocyte apoptosis and evoked extensive reparative responses in the liver, including marked intralobular proliferation of biliary lineage cells and trans-differentiation and proliferation of the oval cells. However, division of pre-existing hepatocytes was significantly diminished in HR-Csn8KO livers. These findings indicate that Csn8 is essential to the ability of mature hepatocytes to proliferate effectively in response to hepatic injury. The histopathological examinations revealed striking hepatocytomegaly in Csn8-deficient livers. The hepatocyte nuclei were dramatically enlarged and pleomorphic with hyperchromasia and prominent nucleoli, consistent with dysplasia or preneoplastic cellular alteration in HR-Csn8KO mice at 6 weeks. Pericellular and perisinusoid fibrosis with distorted architecture was also evident at 6 weeks. It is concluded that CSN8/CSN is essential to postnatal hepatocyte survival and effective proliferation.
Cell Death and Differentiation (2011) **18,** 259–270; doi:10.1038/cdd.2010.98; published online 6 August 2010

The COP9 signalosome (CSN) was originally identified as a developmental regulator in *Arabidopsis thaliana*, and was subsequently found to be highly conserved in animals.[1] The CSN holocomplex consisting of eight unique subunits (CSN1 through CSN8) in higher eukaryotes displays significant homologies to the lid subcomplex of 26S proteasomes.[2] CSN has an isopeptidase activity. It physically interacts with cullin-RING E3 ligases (CRLs) and removes ubiquitin-like protein Nedd8 from cullin (Cul) in a reaction known as deneddylation.[3] This activity, along with the specifically associated de-ubiquitinase UBP12/USP15, enables CSN to regulate the assembly, stability and activity of various CRLs.[3–6]

Genetic and molecular dissections of CSN has revealed its versatility in regulating a diverse set of cellular and developmental processes including development,[7–11] cell cycle progression,[8,12–15] DNA damage repair,[16] immune responses,[8,9,17] cell death and transcription control.[7,18–21] The pleiotropic functionalities of the CSN may be attributed, in part, to the dynamic assembly of CSN mini-complexes.[22,23]

Germ-line gene targeting in mice has shown that the deletion of the *csn2*, *csn3*, *csn5 or* c*sn8* is embryonically lethal,[8,24–26] which in some cases is accompanied with elevated levels of p53 and p27.[27] In the case of c*sn5* knockout, massive apoptosis has been reported.[26] To investigate CSN (patho)physiological significance, conditional gene targeting in mice has recently been achieved. This approach has so far been successfully used in investigating the functions of Csn8 and Csn5 in T-cell development.[8,9] The *in vivo* physiological significance of CSN in other organs or cell types in intact vertebrate animals remains unclear.

The liver is a multifunctional organ that has essential roles in metabolism, biosynthesis, secretion, excretion and detoxification. The basic functional unit of the liver is the hepatic lobule, which consists of hepatocyte plates radiating outward from a central vein. As the parenchymal cells of the liver, hepatocytes constitute approximately 80% of the liver mass. The chief intralobular non-parenchymal cells are the epithelia lining the sinusoidal capillary between hepatocyte plates. The biliary epithelial cells form a delicate biliary drainage system that collects bile secreted from hepatocytes at the periphery of hepatic lobules. The hepatic progenitor cells (e.g., oval cells) are believed to originate from the biliary lineage. Importantly, the liver can regenerate to compensate for lost tissue primarily by proliferation of the pre-existing hepatocytes or by proliferation of liver progenitor cells if pre-existing hepatocytes are unable to proliferate effectively.[28–29] The capacity of hepatic

[1]Division of Basic Biomedical Sciences, Sanford School of Medicine of the University of South Dakota, Vermillion, SD, USA; [2]Cardiovascular Research Institute, Sanford School of Medicine of the University of South Dakota, Vermillion, SD, USA; [3]Department of Pathology and Laboratory Medicine, University of Rochester Medical Center, Rochester, NY, USA and [4]Department of Molecular, Cell, and Developmental Biology, Yale University, New Haven, CT, USA
*Corresponding author: X Wang, Division of Basic Biomedical Sciences, Sanford School of Medicine of the University of South Dakota, 414 East Clark Street, Lee Medical Building, Vermillion, SD 57069, USA. Tel: +605 677 5132; Fax: +605 677 6381; E-mail: Xuejun.Wang@usd.edu
Keywords: COP9 signalosome; CSN8; hepatocytes; liver regeneration; conditional gene targeting
Abbreviations: CSN, COP9 signalosome; HR-Csn8KO, hepatocyte-restricted *Csn8* knockout; CRLs, cullin-RING E3 ligases; Cul, cullin; TUNEL, terminal deoxynucleotidyl transferase dUTP nick end labeling; ALT, alanine transaminase; AST, aspartate transanminase; GS, glutamine synthetase; Apo, apolipoprotein A-I; FBN, fibrinogen β; TTR, transthyretin; CDK, cyclin-dependent kinase; PCNA, proliferating cell nuclear antigen; pRb, retinoblastoma protein; CK19, cytokeratin 19; M2PK, M2-type pyruvate kinase
Received 12.1.10; revised 17.6.10; accepted 05.7.10; Edited by M Piacentini; published online 06.8.10

repopulation after tissue loss can maintain tissue homeostasis but also constitutes the pathological basis of various liver diseases. Therefore, investigating the functional significance of the CSN in postnatal livers may allow us to gain insights into the role of the CSN in cell cycle control and liver regeneration in intact animals.

We have conditionally targeted the *csn8* gene in hepatocytes in mice using the *Cre-loxP* system. The characterization of resultant mice with hepatocyte-restricted *csn8* knockout (HR-Csn8KO) reveals that in the absence of Csn8, hepatocytes displayed striking morphological changes and massive apoptosis. The injury resulting from HR-Csn8KO led to marked proliferation of the oval cells and cells of the biliary lineage, and extensive pericellular and perisinusoid matrix deposition, a hall mark of liver fibrosis. The HR-Csn8KO-induced changes recapitulate the sequalea of chronic hepatic injury such as chronic viral hepatitis. It is concluded that Csn8/CSN is required for the survival and effective proliferation of postnatal mature hepatocytes and thereby is essential to postnatal hepatocyte homeostasis.

Results

Establishment and temporal characterization of HR-Csn8KO. We conditionally ablated the *csn8* gene in hepatocytes in mice using the *Cre-loxP* system. The recently established *csn8*$^{flox/flox}$ mice were cross-bred with a previously described hepatocyte-restricted mouse model, which expresses Cre recombinase under the control of an albumin promoter (Alb-Cre$^+$).[8,30] The cross-breeding gave rise to the following four genotypes at the expected Mendelian ratio at birth (Figure 1a): Csn8$^{flox/flox}$::Alb-Cre$^+$, Csn8$^{flox/flox}$::Alb-Cre$^-$, Csn8$^{flox/+}$::Alb-Cre$^+$ and Csn8$^{flox/+}$::Alb-Cre$^-$, indicating that

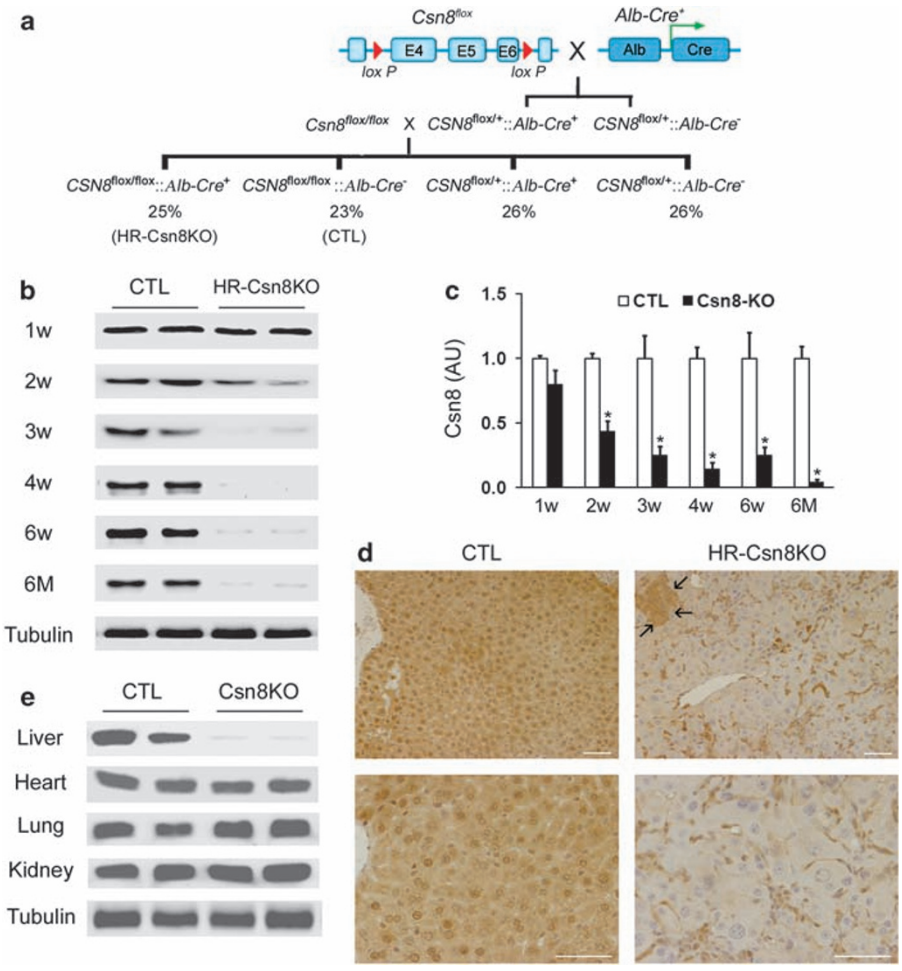

Figure 1 Postnatal HR-Csn8KO. (**a**) An illustration of the breeding strategy to generate CSN8$^{flox/flox}$::Cre (+) mice. The Cre transgene expression is under the control of an albumin promoter. CSN8$^{flox/flox}$::Cre(+) mice are referred to as Csn8KO while littermate CSN8$^{flox/flox}$::Cre(−) mice were used as controls (CTL). The percentage distribution of different genotypes was derived from a total of 247 littermates at 8–10 days of age. (**b**, **c**) Western blot analyses of temporal changes in Csn8 protein levels in the liver. Total liver protein extracts were used for the analyses. The level of β-tubulin was examined for loading control (the same for other panels or figures). At each time point, livers of four mice per group were examined. (**d**) Representative images of Csn8 immunohistochemistry (brown) of liver tissues from 6-week-old mice. The nucleus is counter stained with hematoxylin. Scan bar = 50 μm. Arrows point to a small island of hepatocytes that are Csn8-positive. (**e**) Csn8 protein expression in indicated organs at 6 weeks of age. AU: arbitrary unit; mean ± S.D. are presented; compared with CTL, $^*P<0.01$ *versus* CTL

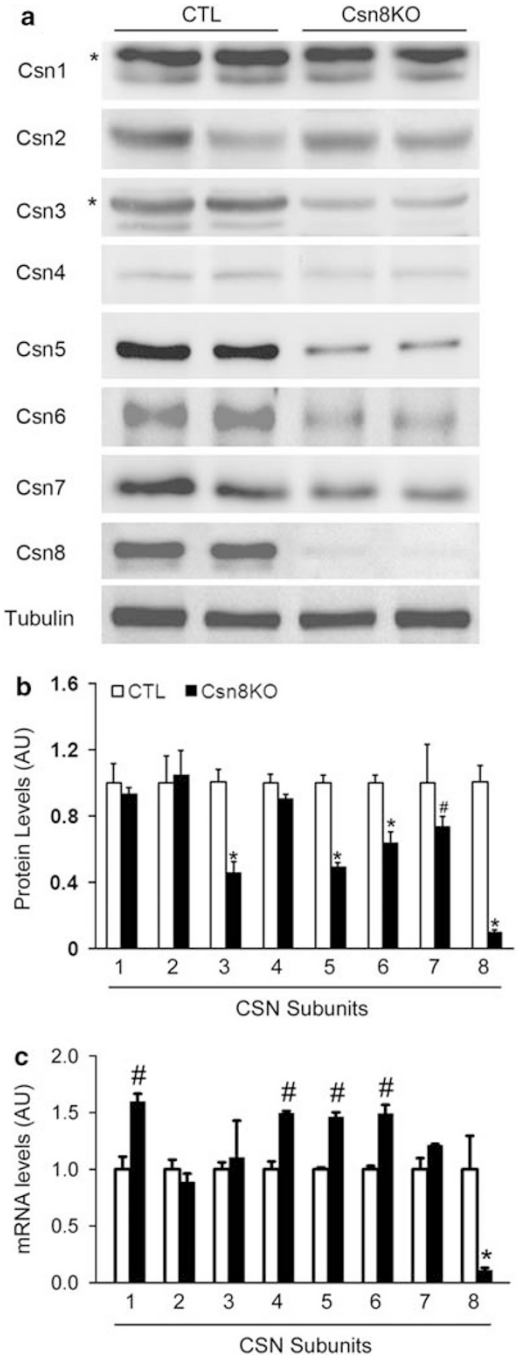

Figure 2 Changes in the expression of CSN subunits in HR-Csn8KO livers from 4-week-old mice. (**a**) Representative western blot images of eight CSN subunits. β-Tubulin is probed as loading control. (**b**) A summary of densitometric data of western blots ($n=4$ mice per group). (**c**) Changes in the mRNA levels of each CSN subunit. Total RNA was extracted from mouse liver tissue ($n=4$ mice per group) and used for measuring mRNA levels of CSN subunits with reverse-transcription (RT-) PCR. For each liver RNA sample, one reverse transcription reaction was performed to generate the first strand cDNA for all subsequent PCR's. For each gene, trials were carried out using various known amounts of the same template derived from a CTL RNA sample to determine the optimal PCR cycle number. GAPDH was co-amplified with each CSN subunit via duplex PCR. GAPDH signal was then used to normalize the co-amplified CSN subunit signal for the quantification. The mean value of the density ratios between a CSN subunit and co-amplified GAPDH of the CTL group is set as one arbitrary unit (AU) and used to convert all density ratios to AU values of the CSN subunit, $^{*}P<0.01$, $^{\#}P<0.05$ *versus* CTL

all genotypes were viable. We examined Csn8 protein levels in the liver of $Csn8^{flox/flox}$::Alb-Cre^{+} and $Csn8^{flox/flox}$::Alb-Cre^{-} littermate mice, at 1, 2, 3, 4 and 6 weeks and 6 months after birth (Figures 1b and c). Liver Csn8 protein levels began to significantly decrease at 2 weeks after birth and continued to decrease afterward, reaching the lowest level at 4 weeks. The decreased expression of Csn8 in liver was maintained for as long as 6 months. Our initial analyses revealed that liver Csn8 protein levels at 4 weeks were not significantly different among $Csn8^{+/+}$::Alb-Cre^{-}, $Csn8^{+/+}$::Alb-Cre^{+}, $Csn8^{flox/flox}$::Alb-Cre^{-} and $Csn8^{flox/+}$::Alb-Cre^{-} mice. Therefore, we chose $Csn8^{flox/flox}$::Alb-Cre^{-} littermate mice to be the control (CTL) for $Csn8^{flox/flox}$::Alb-Cre^{+} (HR-Csn8KO) mice for subsequent experiments. It is noteworthy that $Csn8^{flox/flox}$::Alb-Cre^{-} and $Csn8^{flox/+}$::Alb-Cre^{+} littermate mice are phenotypically indistinguishable.

To verify the cell-type specificity of the Csn8 knockout, immunohistochemical staining for Csn8 was performed (Figure 1d). In CTL livers, Csn8 is expressed in both hepatocytes, which have large round nuclei, and non-hepatocytes. In hepatocytes, Csn8 is distributed in both cytoplasm and the nucleus, with a higher concentration in the latter. In HR-Csn8KO livers, however, over 90% of hepatocytes are negative for Csn8 protein while all the non-hepatocytes cells remain positive for Csn8. This result shows that the ablation of Csn8 is specific to hepatocytes. Additionally, we found that the morphology of Csn8-negative hepatocytes is heterogeneous, as many of their nuclei are markedly larger than their counter-parts in CTL livers. Interestingly, the Csn8-positive hepatocytes, which account for $<10\%$ of the hepatocyte population in HR-Csn8KO livers tend to be clusters of a few cells (arrows in Figure 1d) with comparable cell size and nuclear size to the hepatocytes in CTL livers.

We examined Csn8 protein levels in other organs. As expected, no changes were detected in the heart, lungs and kidney of HR-Csn8KO mice, compared with the littermate controls (Figure 1e).

Effects of HR-Csn8KO on the protein abundance of other CSN subunits and on Cul neddylation. It has been recently reported that the downregulation of Csn8 by small interference RNA in cultured HEK293 cells or the loss of Csn8 in peripheral T cells resulting from conditional gene targeting leads to differential alterations of the protein levels of other CSN subunits;[8,18] but this has not been examined in a parenchymal organ of vertebrates. Western blot analyses of individual CSN subunits in HR-Csn8KO livers showed that ablation of Csn8 in hepatocytes led to significant reductions in Csn3, Csn5, Csn6 and Csn7, a moderate reduction in Csn4, but had little effect on Csn1 and Csn2 protein levels (Figures 2a and b). These data indicated that loss of Csn8 differentially destabilizes other CSN subunits, demonstrating that Csn8 is necessary for complex integrity in hepatocytes. This is further supported by the measurement of the steady-state mRNA levels in the liver, which revealed that the mRNA levels of none of the other 7 CSN subunits were decreased but those of Csn1, Csn4, Csn5 and Csn6 were modestly but statistically significantly increased in HR-Csn8KO mice compared with CTL mice (Figure 2c).

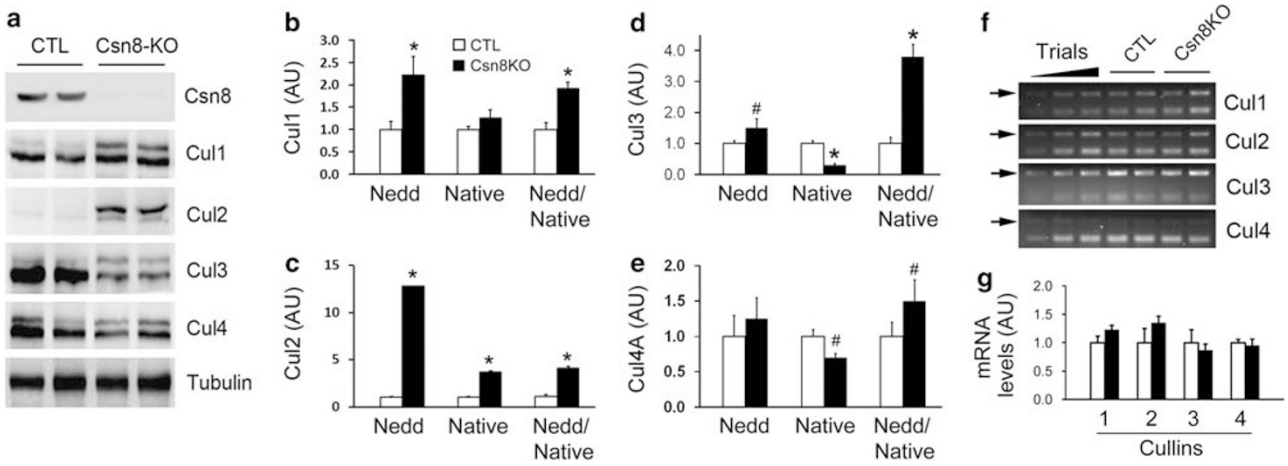

Figure 3 Changes in the expression of Culs in HR-Csn8KO livers at 4 weeks of age. (**a**–**e**) Western blot analyses for the indicated Culs. Representative western blot images of the neddylated (the upper band) and native forms of indicated Culs are shown in panel (**a**). Bar graphs show quantitative changes in the abundance of the neddylated form (Nedd), the native form (Native) and the neddylated form/native form ratio (Nedd/Native) of Cul 1 (**b**), Cul 2 (**c**), Cul 3 (**d**) and Cul 4A (**e**). For each parameter, the mean value of the CTL group was set as one arbitrary unit (AU) and utilized to normalize the corresponding HR-Csn8KO group. (**f**, **g**) RT-PCR analyses show no change in Cul mRNA levels. Trials to determine the optimal PCR cycle number for a given gene and the co-amplification of GAPDH with each Cul member via duplex RT-PCR's were performed as described in Figure 2c. Representative gel images of the indicated RT-PCR products are shown in panel (**f**) in which the images of the 'Trials' determining the optimal number of PCR cycles are also included. The quantitative results from four mice of each group are summarized in panel (**g**), $^{*}P<0.01$, $^{\#}P<0.05$ *versus* CTL

Deneddylation of Cul family of proteins is a *bona fide* activity of the CSN holocomplex. To monitor the activity of the CSN, we examined the levels of native and neddylated forms of Culs in HR-Csn8KO livers. In all cases, HR-Csn8KO livers contained increased levels of neddylated form of Cul proteins compared with the CTL group (Figures 3a–e), indicating a defect in deneddylation. This phenotype is commonly found in all of the lose-of-function mutants of a CSN subunit.[1] Interestingly, different Cul members showed distinct changes in overall protein abundance (Figures 3a–e) although their mRNA levels were not significantly changed (Figures 3f and g). Most strikingly, Cul2 level was drastically elevated, and was predominantly accumulated in the neddylated form (Figures 3a and c). In contrast, Cul3 abundance significantly declined (Figures 3a and d) on Csn8 ablation. Native Cul1 remained unchanged but neddylated Cul1 clearly increased. Cul4 did not drastically change in abundance. These results show that Csn8 is required for maintaining the normal modification dynamics and the abundance of multiple Culs.

Csn8-null hepatocytes show unique morphology. In normal livers, the centrally located hepatocyte nucleus is round and relatively large but the nuclei of non-hepatocyte cells usually have elongated, oval or irregular shapes, and are relatively small and associated with less cytoplasm.[31,32] These morphological characteristics make it easy to distinguish hepatocytes from non-hepatocyte cells in liver tissue sections. Hematoxylin-eosin (H-E) staining of liver tissue sections revealed notable histological lesions in HR-Csn8KO mouse livers at 6 weeks (Figure 4). The major pathological lesions include striking hepatocytomegaly and marked pleomorphism (Figure 4, open arrows). The hepatic nuclei were enlarged and pleomorphic with hyperchromasia, prominent nucleoli and altered nuclear to cytoplasmic ratios in the basophilic and/or clear cells. In addition, non-parenchymal cells were significantly increased in abundance. These are consistent with dysplasia or preneoplastic hepatic lesions during early postnatal liver growth and development.

CSN8 is essential to hepatocyte survival and liver function. To better understand the physiological significance of Csn8/CSN in hepatocyte survival, we examined apoptosis prevalence and caspase activation. Terminal deoxynucleotidyl transferase dUTP nick end labeling (TUNEL) was used to detect DNA fragmentation. Compared with littermate controls, TUNEL-positive cells were more than doubled in HR-Csn8KO livers at 4 weeks ($P<0.01$; Figures 5a and b). Consistent with increases in apoptosis, the cleaved (i.e., activated) forms of both caspase 3 (Figures 5c and e) and caspase 9 (Figures 5c and d) were markedly increased in HR-Csn8KO livers.

HR-Csn8KO livers were larger and showed a greater liver weight/body weight (LW/BW) ratio than their littermate CTL at 6 weeks (Figures 6a and b). Liver enlargement is usually an indicator of certain liver malfunctions. We determined serum alanine transaminase (ALT) and aspartate transanminase (AST) activities of HR-Csn8KO mice at 6 weeks. HR-Csn8KO mice showed moderate, but statistically significant increases of both activities (Figure 6b), indicating that the liver is injured by HR-Csn8KO. To further examine liver function, the mRNA and protein expression of representative liver genes: glutamine synthetase (GS), apolipoprotein A-I (Apo), fibrinogen β (FBN) and transthyretin (TTR) in the liver tissue, as well as their protein levels in the plasma, were assessed at 6 weeks of age. The steady-state mRNA levels of GS, Apo, FBN and TTR in the liver tissue (Figures 6c and d) and their protein levels in plasma (Figures 6g and h) were all significantly lower in the HR-Csn8KO mice than the CTL mice ($P<0.05$, 0.01). The protein levels of GS, Apo and FBN were also significantly

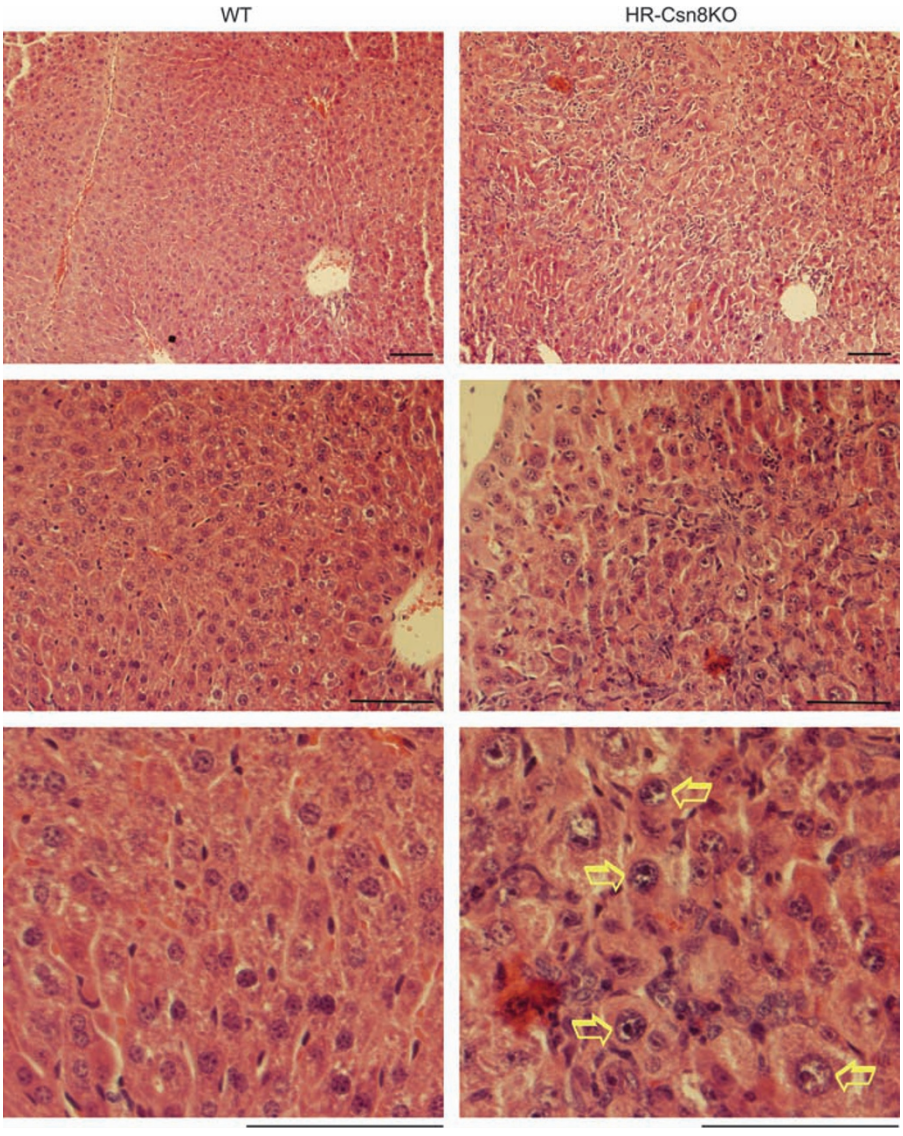

Figure 4 Histopathology of HR-Csn8KO livers. Liver tissue samples from mice of 6 weeks of age were fixed by 10% formalin and processed for paraffin sectioning and H-E staining. Liver dysplasia or preneoplastic cellular alteration is evident. Striking hepatocytomegaly and marked pleomorphism were also observed. The hepatic nuclei (open arrows) were enlarged and pleomorphic with hyperchromasia and prominent nucleoli. Non-hepatocyte population was significantly increased. Four representative regions of three livers per group were examined. The images presented are representative to each group. Scale bar $=120\ \mu$m

decreased while TTR was modestly increased in the liver of the HR-Csn8KO mice, compared with the CTL group (Figures 6e and f). Taken together, these liver gene expression data show that liver function is impaired by HR-Csn8KO. The cause for the increased TTR protein levels in HR-Csn8KO livers is unclear at this point. Given its decreased mRNA levels in the liver and decreased protein levels in the plasma of HR-Csn8KO mice, a defect in TTR secretion and/or an increase in TTR protein stability in Csn8-deficient hepatocytes can conceivably be the suspects.

We further tested the ability of HR-Csn8KO mice to cope with loss of liver mass. After surgical resection of two-thirds ($\sim$67%) of the liver, we found all three HR-Csn8KO mice died within 12-h postoperation while all three CTL littermates survived 72 h after the surgery.

Increased cell proliferation in HR-Csn8KO livers. Normally, mature liver exhibits minimal cell proliferation activities because hepatocyte turnover rate is very low.[28] Analyses of the expression of the key G1 phase regulators (Figures 7a–d) revealed that the expression of CDK4, CDK6, and both activated (Thr286-phosphorylated form) and total cyclin D1 were significantly increased in HR-Csn8KO livers. Phosphorylation of retinoblastoma protein (pRb) at Ser790 (p-pRb) and, to a less extent, the level of total pRb were also significantly elevated in the HR-Csn8KO liver. Hypo-phosphorylated Rb binds and inhibits transcription factor E2F.[33] The phosphorylation inactivates Rb proteins and releases E2F, which becomes available for stimulating the expression of proliferation-specific target genes, such as the proliferating cell nuclear antigens (PCNAs). Indeed, a

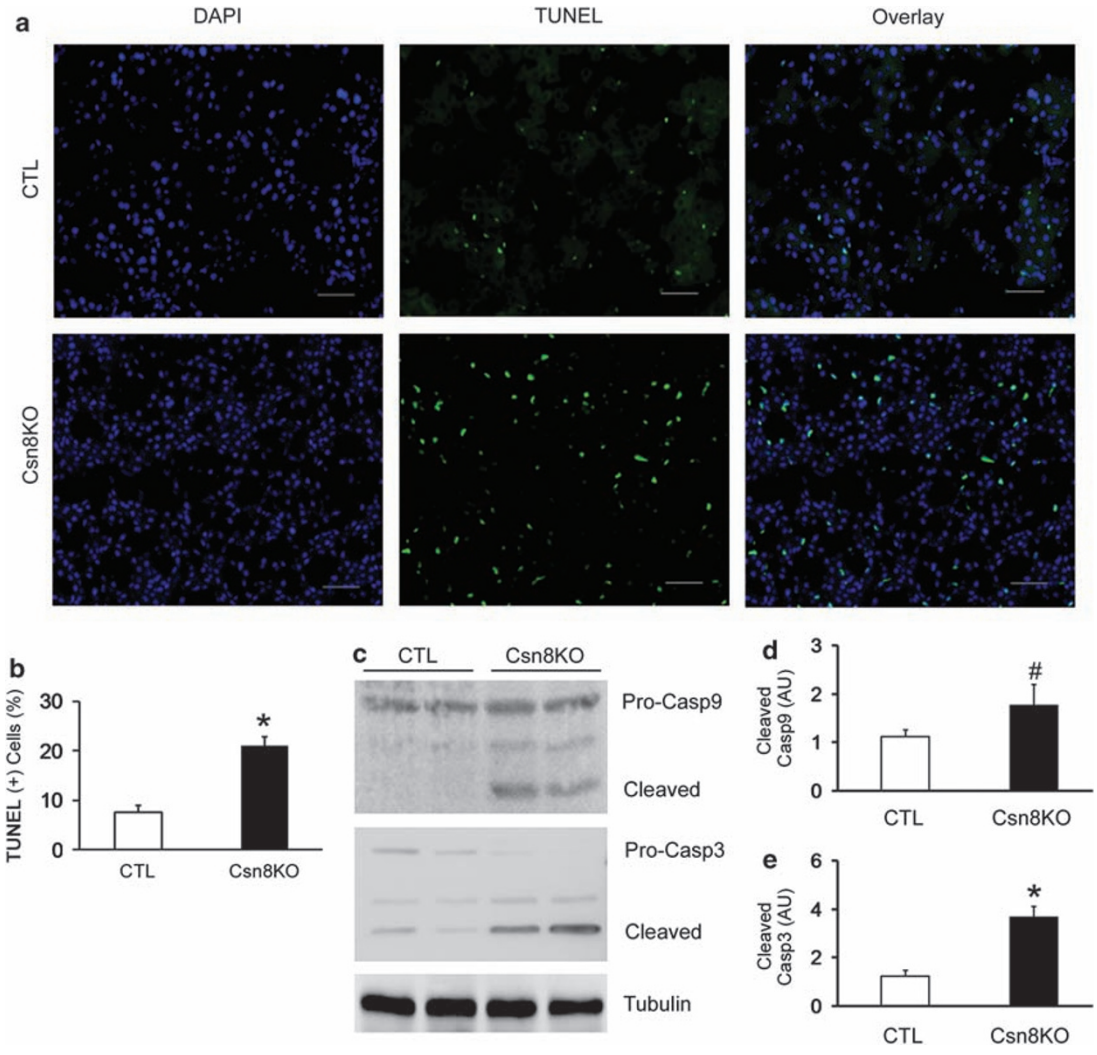

Figure 5 Apoptosis is induced in HR-Csn8KO livers. (**a**) Representative images of TUNEL staining of liver tissue cryosections from 4-week-old mice. Scan bar $= 50\ \mu$m. (**b**) A summary of the prevalence of TUNEL-positive cells. Four livers per group and 300 cells from each liver were counted. (**c**–**e**) Western blot analyses of caspases 9 and 3 in liver tissue at 4 weeks. Representative images (**c**) and quantitative changes in the abundance of cleaved caspases 9 (Casp9, **d**) and 3 (Casp3, **e**) are shown, $^{*}P<0.01$, $^{\#}P<0.05$ *versus* CTL

progressive increase in PCNA protein expression was detected in the liver following HR-Csn8KO (Figures 7e and f). These results show that, unlike normal mature liver, HR-Csn8KO liver displays a gene expression pattern normally associated with actively proliferating cells.

Hepatic progenitor cells in HR-Csn8KO livers are induced to undergo cell proliferation. We reasoned that the cell proliferation program is activated in HR-Csn8KO livers in part to compensate for the loss of hepatic tissue because of increased apoptotic cell death (Figure 5). Normally, the mature hepatocytes are activated to re-enter the cell cycle, undergo proliferation and effectively repair the loss of liver mass. However, if the hepatocytes are impaired in cell division, liver progenitor cells, such as oval cells and biliary epithelia will be induced to proliferate for repairment.[28,29]

To investigate the cell-type identity of the proliferating cells in HR-Csn8KO livers, we carried out immuno-staining for Ki67, a classic marker of cell proliferation, on tissue sections (Figure 8). On the basis of nuclear shape and the amount of cytoplasm, it is clear that most of the Ki67-positive cells from the HR-Csn8KO sample were non-hepatocytes and only a small percentage ($<10\%$) of the Ki67-positive cells appeared to be from the pre-existing mature hepatocytes (marked by arrows in Figure 8). The mass majority of these Ki67-positive hepatocytes displayed a nuclear morphology virtually indistinguishable from that of normal mature hepatocytes from the control liver (arrows, Figure 8), while very few of the typical Csn8-null hepatocytes, which have enlarged nuclei, were Ki67-positive (open arrow, Figure 8) although Csn8-null hepatocytes account for the majority of the hepatocyte population. As most proliferating hepatocytes in HR-Csn8KO livers did not show the nuclear phenotype associated with Csn8 ablation, we speculate that those cells were not completely deplete of Csn8 yet.

As mentioned above, non-hepatocyte cells constituted the major proliferating population in HR-Csn8KO livers. To identify their cell types, we first determined whether they are of

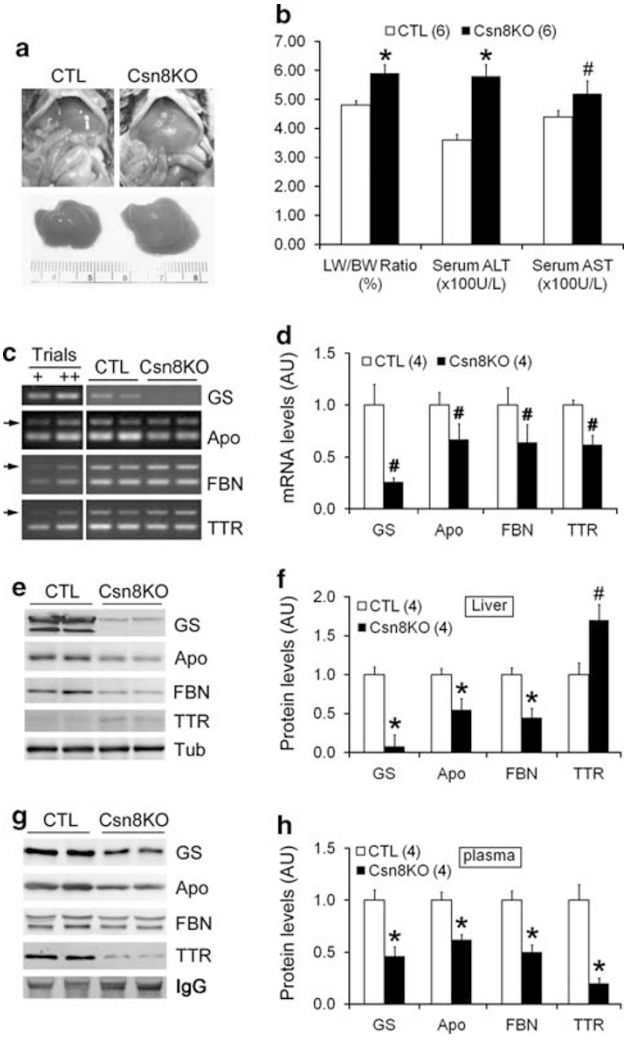

Figure 6 Characterization of liver gross morphology and liver function. (**a**, **b**) Changes in liver size at 6 weeks and the serum aminotransferas activity (ALT and AST, **b**) at 3 weeks of age. LW, liver weight; BW, body weight. $N = 6$ mice per group. (**c**, **d**) Changes in the mRNA levels of GS, Apo, FBN and TTR in the liver tissue at 4 weeks of age. Duplex RT-PCR's between GAPDH and the indicated gene were performed as described in Figure 2c. The PCR primers for GS were not suitable for duplex PCR with GAPDH; therefore, the loading control of GS mRNA quantification used the pooled GAPDH signals from its co-amplifications with Apo, FBN and TTR of the same sample. (**e**–**h**) Western blot analyses for the protein levels of GS, Apo, FBN and TTR in the liver (**e**, **f**) and plasma (**g**, **h**) at 4 weeks. β-Tubulin (Tub) and IgG in liver tissue (**e**) and plasma samples (**g**), respectively were probed as loading controls, $^{*}P < 0.01$, $^{\#}P < 0.05$ *versus* CTL

the biliary epithelial lineage, the main source of liver progenitor cells. We immunolabeled for cytokeratin 19 (CK19), a specific intermediate filament protein of biliary epithelia.[34] Strikingly, the intra-lobular CK19-positive cells were increased from $<0.5\%$ in the littermate CTL livers to $>20\%$ of total cell population in HR-Csn8KO livers (Figure 9c). Furthermore, double-immunolabeling for Ki67 and CK19 revealed that most Ki67-positive cells are also CK19-positive in HR-Csn8KO livers (Figure 9b), whereas the Ki67-positive hepatocytes induced by partial hepatectomy in CTL mice were negative for CK19 (data not shown).

Oval cells represent another major source of hepatic progenitor cells.[35] They can be identified by the M2-type pyruvate kinase (M2PK) marker. We performed double immunofluorescence labeling for Ki67 and M2PK to determine whether the oval cells in HR-Csn8KO livers can proliferate (Figure 10). In CTL livers, scattered M2PK-positive cells were observed but none of them were positive for Ki67. However, in livers with HR-Csn8KO a large number of M2PK-positive cell are frequently clustered with Ki67-positive cells. Many of them are M2PK and Ki67 double-positive, revealing active proliferation of oval cells in HR-Csn8KO livers (Figure 10).

Together these results indicate that biliary epithelia and oval cells, rather than mature hepatocytes, contributes most significantly to the proliferating cell population, and likely account for the activation of cell cycle genes in HR-Csn8KO livers.

Liver fibrosis through hepatic stellate cell activation in HR-Csn8KO mice. Hepatic fibrogenesis often accompanies chronic hepatic injury. Masson's trichrome staining was used to examine potential fibrosis in HR-Csn8KO livers. Consistent with the increases in non-parenchymal cells observed with H-E staining (Figure 4), the trichrome staining of liver sections from 6-week-old HR-Csn8KO mice exhibited extensive pericellular and perisinusoid fibrosis (Figure 11a). We also examined the molecular changes that associated with fibrosis. We found that the mRNA expression of transforming growth factor β1, a potent profibrogenic cytokine that has a key role in promoting fibrogenic responses,[36] was upregulated about fourfold in HR-Csn8KO livers, compared with the control livers (Figures 11b and c). Moreover, western blot analyses revealed a significant increase in the expression of desmin, which is a marker of activated hepatic stellate cells/myofibroblasts (Figures 11d and e). These results together indicate that HR-Csn8KO causes extensive liver fibrosis.

Discussion

The physiological significance of the CSN in a specific organ of vertebrates has only been studied for T-cell development and activation.[8,9] Through conditionally targeting, the *csn8* gene in hepatocytes in mice, this study represents the first investigation of the function of a *CSN* gene in a parenchymal organ of vertebrates using a loss-of-function approach. We have found that Csn8 is necessary for Cul deneddylation and for structural integrity of CSN holocomplex. Deficiency of Csn8 differentially affects the stability of other CSN subunits. We have also discovered that Csn8/CSN is essential to hepatocyte survival and maintaining normal liver function. Postnatal HR-CSN8KO triggered a spontaneous robust reparative response in liver, including proliferation and transdifferentiation of hepatic progenitor cells, and hepatic fibrogenesis through activation of hepatic stellate cells. We demonstrate these changes at both the cellular and molecular levels.

HR-Csn8KO triggers robust proliferation of hepatic progenitor cells rather than mature hepatocytes. In spite of the prevalent cell death (Figure 5), we were curious to find that HR-Csn8KO livers exhibit only moderate

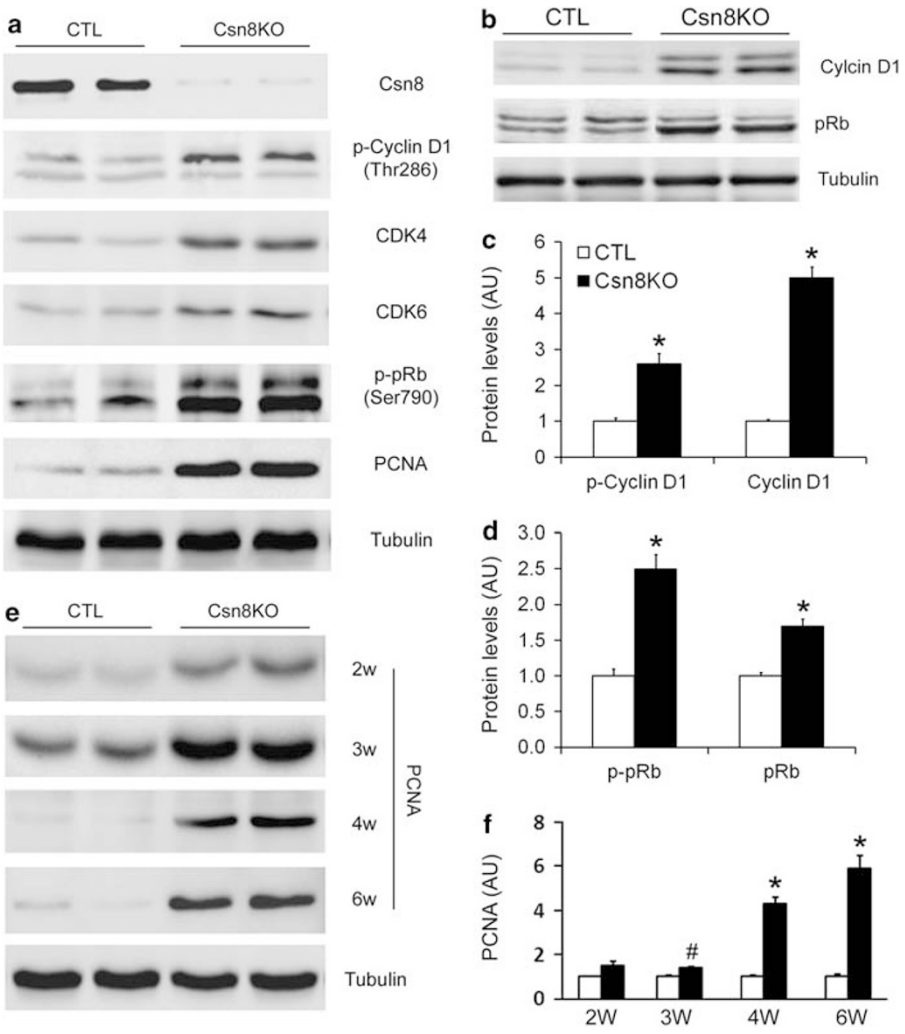

Figure 7 Western blot analyses for cell cycle regulators in livers with HR-Csn8KO. (**a**–**d**) Activation of the cyclin D1/pRb signaling at 6 weeks. (**e**, **f**) Increases in protein expression of the PCNA in HR-Can8KO livers over the first 6 postnatal weeks (W), $^{*}P<0.01$, $^{\#}P<0.05$ *versus* CTL

functional deficiency based on the increases in liver size and serum ALT and AST activities as well as moderately decreased expression of representative liver genes (GS, Apo, FBN and TTR, Figure 6). Our data suggest that HR-Csn8KO livers underwent rigorous repair in the few weeks following Csn8 ablation, to cope with the tissue loss from the cell death.

Most adult hepatocytes withdraw from the cell cycle and stay in a quiescent state. However, a reduction in functional liver mass by either chemically induced hepatotoxic injury or surgical resection evokes a rapid proliferative response to replenish the liver parenchyma and restore liver function.[28] In adult animals, at least in rodents, liver regeneration is mainly carried out by proliferation of pre-existing hepatocytes rather than hepatic progenitor cells unless the ability of hepatocytes to proliferate is severely inhibited.[28,31]

HR-Csn8KO started in between postnatal week 1 and 2 and reached the peak at week 4 (Figure 1b) when most, if not all, hepatocytes are fully differentiated and mature. Csn8 was absent in approximately 90% of the mature hepatocytes (Figure 1d). This is consistent with the previously described recombination characteristics of the *Cre* transgenic mouse line used in this study.[30,37] Loss of Csn8 in these hepatocytes caused a markedly higher rate of cell death, and consequently triggered extensive cell renewal in HR-Csn8KO livers (Figures 7–10). Normally, the loss of mature hepatocytes stimulates cell cycle reentry of the remaining mature hepatocytes. However, we found in HR-Csn8KO livers, progenitor cells such as biliary epithelial cells (CK19-positive) and the oval cells (M2PK-positive) are mobilized to undergo robust proliferation as indicated by Ki67 immunoreactivities (Figures 9 and 10). In contrast, no significant cell proliferation of these cell types was detected in wild-type livers, even after partial hepatectomy (data not shown). These results imply that the mature hepatocytes of the HR-Csn8KO liver are unable to effectively proliferate. As Csn8 is deleted only in hepatocytes but not liver progenitor cells (Figure 1d), these findings suggest that Csn8/CSN is required for mature hepatocytes to proliferate effectively. Supporting this notion, it was reported that Csn8 is required for cell cycle re-entry of quiescent mouse

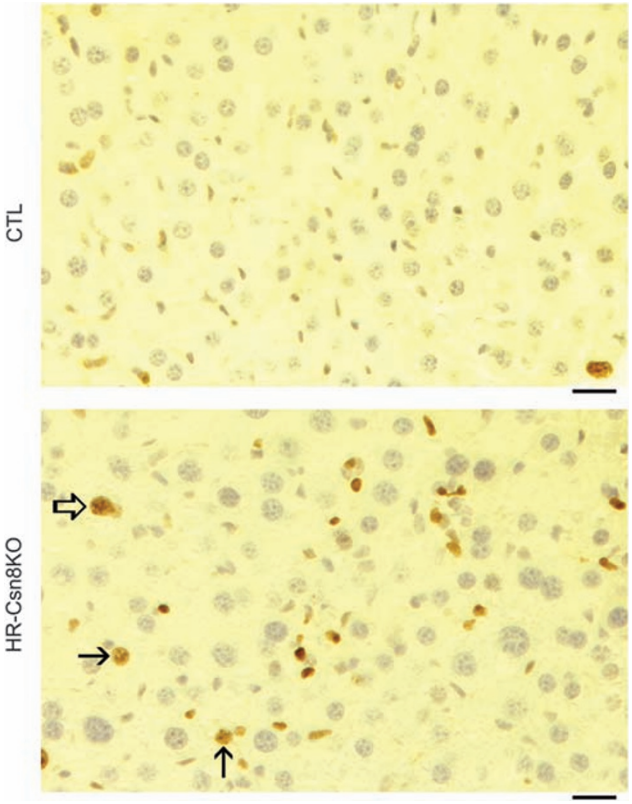

Figure 8 Increased cell proliferation in HR-Csn8KO livers at 6 weeks. Formalin-fixed paraffin-embedded liver tissue sections from CTL and HR-Csn8KO livers were used for immunohistochemical labeling of cell proliferation marker Ki67 (brown). The nucleus was counter-stained with hematoxylin. Representative images are shown. Arrows point to Ki67-positive hepatocytes with normal nuclear morphology. Open arrow points to a Ki67-positive cell with an enlarged nucleus. Scale bar $=50\,\mu$m

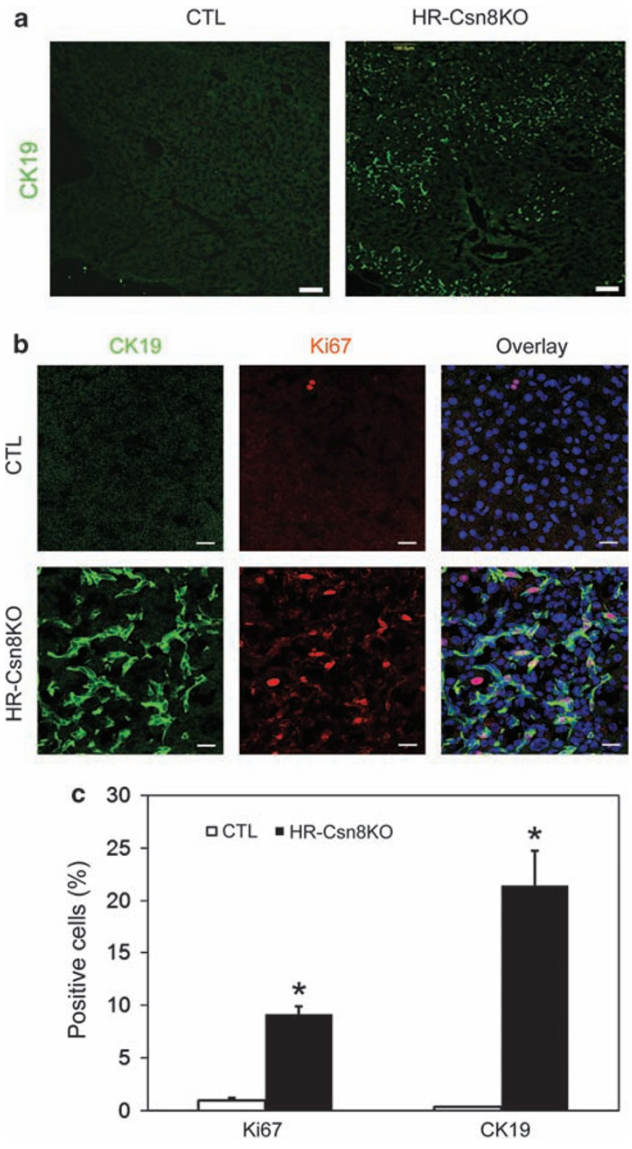

Figure 9 Increased proliferation of biliary lineage cells in HR-Csn8KO livers. (**a**) Representative micrographs showing dramatic increase in the number CK19-positive cells. CK19 is a marker of biliary linease cells. Scale bar $=150\,\mu$m. (**b**) Representative confocal micrographs of double immunofluorescence labeling of Ki67 (red) and CK19 (green). The majority of Ki67-positive cells are positive for CK19. Scan bar $=50\,\mu$m. (**c**) Quantitative comparison of Ki67- or CK19-positive cells between CTL and HR-Csn8KO livers. Three livers per group and 500 cells per liver were analyzed. $^*P<0.01$ *versus* CTL

embryonic fibroblasts and periphery T cells.[8] The ineffectiveness of existing hepatocyte proliferation in HR-Csn8KO livers may be at least partially mediated by the derangement of Culs (Figure 3) because conditional ablation of Cul4A was recently shown to lead to hepatocyte proliferation defects following liver injury in mice.[38]

A small percentage of Ki67-positive cells in HR-Csn8KO livers are indeed of hepatocyte type. However, as the majority of them do not display the characteristic Csn8-minus cell morphology but instead appear identically to normal hepatocytes from the control liver (Figure 8), we believe that the ablation of *csn8* in these Ki67-positive hepatocytes was either unsuccessful or just newly occurred so that the Csn8 protein had not been depleted when the cell was re-activated into proliferation. Alternatively, the small clusters of Csn8-positive hepatocytes in HR-Csn8KO livers may have resulted from proliferation of the new hepatocytes that were trans-differentiated from progenitor cells such as the oval cells, which still carried *Csn8*.

Csn8 is necessary for liver homeostasis and normal functionality. The progenitor cell-mediated liver regeneration proves to be quite powerful, because it apparently compensates fairly well for the massive hepatocyte apoptosis induced by Csn8 ablation such that the HR-Csn8KO mice could live for at least one year (the longest length that the mice were kept).In contrast, the repair is incomplete and not without adverse consequence because severe fibrosis is observed as early as 6 weeks of age (Figure 11). Moreover, our pilot studies on the ability of HR-Csn8KO mice to cope with additional loss of liver function revealed that after surgical resection of two-thirds ($\sim$67%) of the liver, all three HR-Csn8KO mice died within 12-h postoperation while all three CTL littermates survived 72 h after the surgery. Thus, although a highly resilient organ like

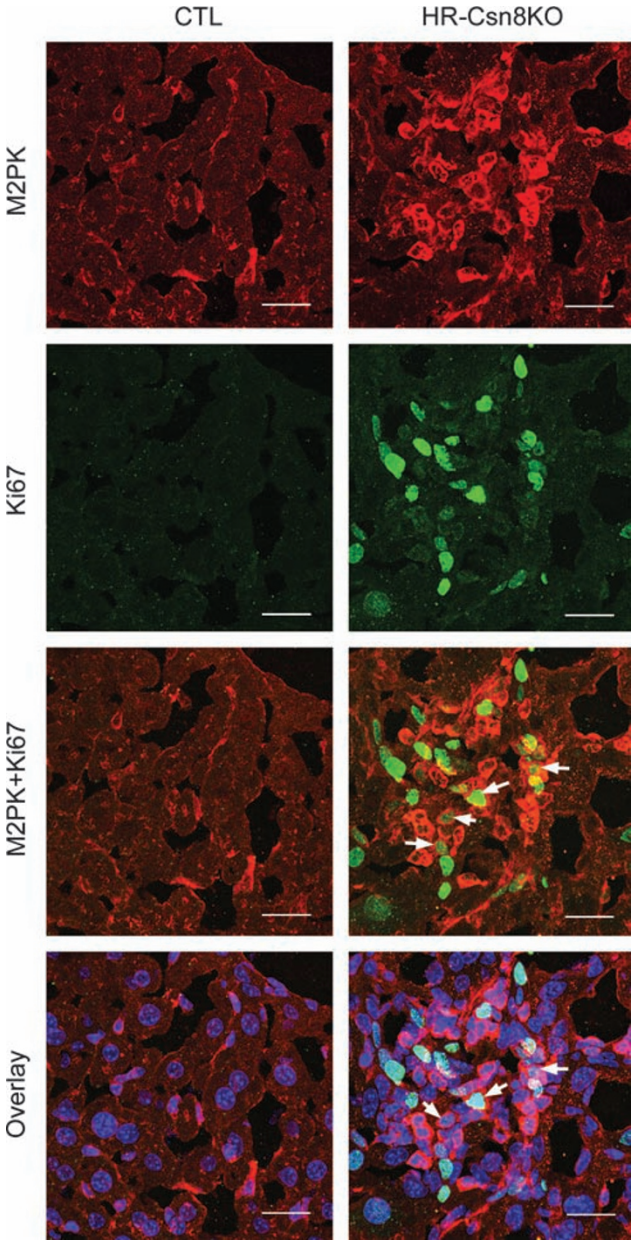

Figure 10 Proliferation of the oval cells in HR-Csn8KO livers. Representative confocal micrographs of double immunofluorescence labeling for M2PK (red) and Ki67 (green) with the nuclear DNA being labeled with DAPI (blue) of liver tissue cryo-sections of CTL and HR-Csn8KO mice are shown. Arrows indicate examples of Ki67 and M2PK double-positive cells in a M2PK-positive niche. Three livers were examined for each group. Scale bar $=25\,\mu$m

the liver may appear fairly normal when Csn8 is deleted from its parenchymal cells, catastrophic results can happen to these animals under adverse conditions.

In summary, this study demonstrates for the first time that Csn8/CSN is required for the survival and effective proliferation of postnatal hepatocytes. Loss of Csn8/CSN function in hepatocytes results in hepatocyte death in the form of apoptosis, evokes robust cell proliferation of the biliary lineage, and leads to extensive hepatic fibrogenesis with

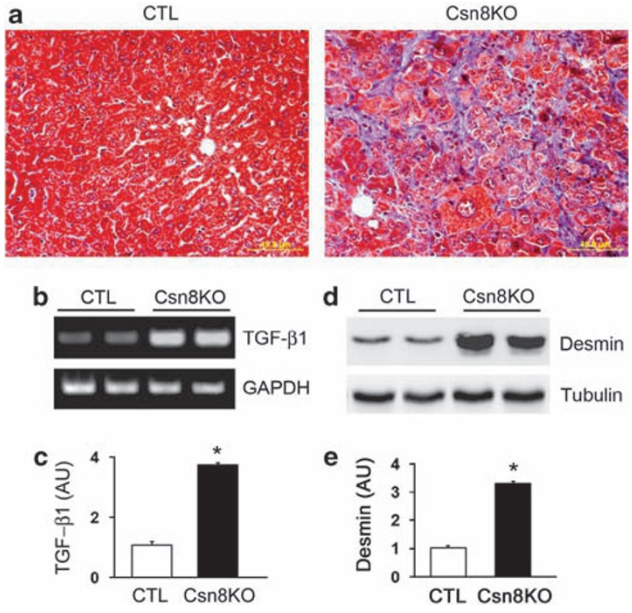

Figure 11 HR-Csn8KO mice develop liver fibrosis. (**a**) Representative Masson's trichrome staining micrographs showing extensive pericellular and perisinusoid matrix deposition in the HR-Csn8KO liver at 6 months. Scale bar $=50\,\mu$m. (**b**, **c**) RT-PCR analysis of TGF-β1 expression in mouse livers. Representative PCR images (**b**) and a bar graph summarizing data from four independent repeats (**c**) are presented. (**d**, **e**) Western blot analyses of desmin protein in mouse livers. Representative images (**d**) and a bar graph summarizing densitometry data from four independent repeats (**e**) are presented. $^*P<0.01$ *versus* CTL

inflammation filtration, hepatic dysplasia or preneoplasmic lesions.

Materials and Methods

Generation of HR-Csn8KO mice and PCR genotyping. Mice used in this study were maintained in the barrier facility according to protocols approved by the ICAUC of the participating institutions. The creation of the mouse line carrying the Csn8-floxed allele ($Csn8^{flox/+}$) was recently reported.[8] We purchased Alb-Cre^+ transgenic mice (*B6.Cg-Tg(Alb-cre)21Mgn/J*) from The Jackson Laboratory (Bar Harbor, ME, USA). In Alb-Cre^+ transgenic mice, the expression of *Cre* recombinase is under the control of an albumin promoter.[30] Using the strategy illustrated in Figure 1a, $Csn8^{flox/+}$ mice or $Csn8^{flox/flox}$ mice were mated with Alb-Cre^+ mice to ultimately obtain littermate compound transgenic mice with a genotype of either $Csn8^{flox/flox}$::Alb-Cre^+ or $Csn8^{flox/flox}$::Alb-Cre^- that were used respectively as the HR-Csn8KO group and the control group (CTL) in this study.

Genomic DNA was isolated from mouse tail clips and amplified by PCR to determine the genotype. Sequences of the sense primer I3F and the antisense primers I6R are respectively 5′-AACAGCTCAGCTGATAAGAGTGG-3′ and 5′-GTAGGTGACCTTCAATGTCAC-3′.

Protein extraction and western blot analysis. Liver tissue samples were homogenized in sample buffer (0.3 M Tris-HCl, pH 6.8, 10% SDS and 5% glycerol) with phosphatase inhibitor cocktail (Sigma, St Louis, MO, USA) and complete protease inhibitor cocktails (Roche, Indianapolis, IN, USA). The protein concentration was determined with BCA reagents (Pierce, Rockford, IL, USA). Equal amounts of proteins were fractionated with SDS-PAGE and transferred to PVDF membranes. For the western blot analyses, the primary antibodies used include antibodies against caspase 9 and caspase 3 (Biomol, Plymouth Meeting, PA, USA), Nedd8 (Alexis), β-tubulin, Desmin (Sigma), CSN1, CSN2, CSN3, CSN4, CSN5, CSN6, CSN7, CSN8 (Biomol), Cul (Cul) 1 and Cul4 (custom made), Cul2 (ZYMED, Carlsbad, CA, USA), Cul3 (Novus, Littleton, CO, USA), cyclin D1,Thr286-phosphorylated cyclin D1, cyclin-dependent kinase (CDK) 4, CDK6,

Table 1 Primers used for RT-PCR

CSN1	Forward	5′-AGATGCTGGACGAGATGAAGGA-3′
	Reverse	5′-TGGATAAGAGCCCGGTTACG-3′
CSN2	Forward	5′-AGCCCAAGACGAACCACTTG-3′
	Reverse	5′-TATACGGCTTGGCCTCTTGTG-3′
CSN3	Forward	5′-AAAACAGCCCCTTCGAGGAA-3′
	Reverse	5′-CTGGCAGAGATCGGCATGTA-3′
CSN4	Forward	5′-AAAGATCTGGCGGGCAAATA-3′
	Reverse	5′-CCATCGCTTCCACAAAAGCT-3′
CSN5	Forward	5′-CAACTTGGAAGTGATGGGTTTG-3′
	Reverse	5′-TCGAGTTTCTGTGCCCTCTACA-3′
CSN6	Forward	5′-CGCTCTTCATCCCCTTGTCA-3′
	Reverse	5′-CCCGATCAGAGCCCCAAT-3′
CSN7	Forward	5′-GACCTTGCATGAGTGGTGTGA-3′
	Reverse	5′-AGTCCGGTGGTGGTTCTCTTT-3′
CSN8	Forward	5′-CTTGCTCCAGAACGACATGA-3′
	Reverse	5′-TGCCATCCTTGTTCCAACAC-3′
Cul1	Forward	5′-AATGTGAGCAGGTCCTCATTGA-3′
	Reverse	5′-TACATGCGGCCCAAATCTTC-3′
Cu2	Forward	5′-GCAGAAGGATACGCCACAAGA-3′
	Reverse	5′-TGCTTTCATGATGCGGACAA-3′
Cul3	Forward	5′-CATCTCATAAATAAGGTGCGAGAAGA-3′
	Reverse	5′-CCATGGCTGTTTGATGATCATT-3′
Cu4	Forward	5′-CTTCCTGTTTCTGGATCGAACCT-3′
	Reverse	5′-GTCGCTGATGATGTGGTTCCT-3′
Apo	Forward	5′-GGCACGTATGGCAGCAAGAT-3′
	Reverse	5′-TAGTCTCTGCCGCTGTCTTTGA-3′
FBN	Forward	5′-GGATGGCAGCGTCGACTTT-3′
	Reverse	5′-TGGCAAGCCACAGTACTTCTTC-3′
TTR	Forward	5′-CCATGAATTCGCGGATGTG-3′
	Reverse	5′-AGCCGTGGTGCTGTAGGAGTA-3′
GS	Forward	5′-CAAGCCCATTCCAGGGAACT-3′
	Reverse	5′-GGCCTCCTCAATGCACTTCA-3′
TGF-β1	Forward	5′-TGACGTCACTGGAGTTGTACGG-3′
	Reverse	5′-GGTTCATGTCATGGAT GGTGC-3′
GAPDH	Forward	5′-GATCGTGGAAGGGCTAATGA-3′
	Reverse	5′-GAGCTCTGGGATGACTTTGC-3′

pRb, Ser790-phosphorylated pRb (Cell Signaling, Danvers, MA, USA), PCNA (AbCam, Cambridge, MA, USA), Apo A-I, FBN (Santa Cruz, Santa Cruz, CA, USA), TTR (Genway, no. 18-202-336039) and GS (GenScript, no. A01305). Horseradish peroxidase-conjugated anti-mouse or anti-rabbit secondary antibodies (Santa Cruz) were used. ECL advanced detection reagents (Amersham Pharmacia Biotech, Piscataway, NJ, USA) were used for detection of the bound secondary antibodies. A VersaDoc Model 4000 Imaging System (Bio-Rad Laboratories, Hercules, CA, USA) was used to visualize and digitalize the western blot images. The densitometry of the western blots was performed with the Quantity-One software (Bio-Rad) as previously described.[18]

Histology, immunohistochemistry and immunofluorescence confocal microscopy. Tissue samples from the right lobe of the liver were fixed in 10% formalin and paraffin embedded. Serial 5-ím paraffin sections were used for conventional H-E staining or Masson's trichrome staining as previously described.[37]

For Csn8 immunohistochemistry, paraffin-embedded sections were deparaffinized and rehydrated. The slides were further incubated in 1N HCl for 8 min at 65 °C and blocked with 0.3%H_2O_2 for 20 min, washed in PBS and blocked with 1% (w/v) bovine serum albumin (BSA) in PBS. Slides were incubated with rabbit anti-Csn8 antibody for 1 h at room temperature. Biotinylated anti-rabbit antibody was used as a secondary antibody at a 1 : 200 dilution and visualized with peroxidase reaction performed with the ABC Vectastain kit (Vector Laboratories, Burlingame, CA, USA).

For immunofluorescence staining, 7-μm sections from frozen tissues were fixed in 4% paraformaldehyde in PBS, permeabilized with 1% Triton X-100 in PBS, blocked with 0.5% BSA solution and incubated overnight with the primary antibody. The unbound primary antibodies were removed by PBS washes (10 min $\times$ 3) before incubation of Alexa Fluor 488 or 568 conjugated appropriate secondary antibodies (Invitrogen, Carlsbad, CA, USA). Double-immunolabeling and subsequent confocal fluorescence microscopy were performed as previously described.[18]

TUNEL assay. To characterize the cell death pattern, DNA fragmentation was detected *in situ* using frozen liver tissue sections and the terminal deoxynucleotidyl transferase (TdT)-mediated dUTP nick-end labeling (TUNEL) assay, according to the manufacturer's instructions of the TUNEL cell death detection kit (Roche Diagnostics, Mannheim, Germany). The label solution only (without terminal transferase) instead of TUNEL reaction mixture was used as the negative control. The negative control images were referenced in determining the level of background subtraction. The nucleus was counter-stained by DAPI. The labeled sections were then observed with a Zeiss Axiovert 200 M epi-fluorescence microscope (Carl Zeiss MicroImaging GmbH, Germany). At least 300 cells were counted from three different representative fields in each liver, and data from four livers per group were analyzed. TUNEL index was expressed as a ratio of the number of positive nuclei and the total number of nuclei revealed by DAPI staining.

Serum ALT and AST activities assays. Blood samples were collected by decollation and centrifuged to obtain the serum. The AST and ALT activities were assayed using ELISA reagent kits from STANBIO Laboratory (Boene, TX, USA).

RNA extraction and RT-PCR. Total RNA was extracted from liver tissue samples using Trizol (Invitrogen) according to the manufacturer's protocol. To measure the relative amount of selected gene transcripts, 1 μg isolated RNA from each sample were reverse transcribed with oligo(dT) primers using Superscript II reverse transcriptase (Invitrogen). One-tenth of the cDNA product was then amplified with gene-specific primers. In all, 20 to 40 cycles of PCR were conducted. PCR products were separated by 2% agarose ethidium bromide gel electrophoresis, imaged and digitized using GelDoc2000 (Bio-Rad) as described.[18] The PCR primers were purchased from Integrated DNA Technologies, Inc. (Coralville, IA, USA) and their sequences are listed in Table 1. Analyses for liver GS and TGF-β1 mRNA levels were done using GAPDH as the quantitative control in which the PCRs for GAPDH and GS or TGF-β1 of the same sample were performed in separate reaction tubes. The assessments of the mRNA levels of all other genes, including each CSN subunit, members of the Cul family, and other representative liver genes (Apo, FBN and TTR) used quantitative duplex RT-PCR in which GAPDH was co-amplified in the same reaction as the gene of interest. In each case, the number of PCR cycles and other PCR conditions were optimized to suit the quantitative purpose using various amount of cDNA templates derived from the same CTL RNA sample.

Statistical methods. All quantitative data are presented as mean $\pm$ S.D. Unpaired Student's *t*-test was used for statistical comparison between the CTL and HR-Csn8KO groups. A *P*-value $<5\%$ is considered statistically significant.

Conflict of interest

The authors declare no conflict of interest.

Acknowledgements. Dr X Wang is an established investigator of the American Heart Association (AHA). This work was supported in part by grants R01HL072166, R01HL085629, and R01HL068936 from the NIH and grant 0740025N from AHA (to XW), and an AHA postdoctoral fellowship (to HS), and by the Physician Scientist Program of the University of South Dakota.

1. Wei N, Deng XW. The COP9 signalosome. *Annu Rev Cell Dev Biol* 2003; **19**: 261–286.
2. Glickman MH, Rubin DM, Coux O, Wefes I, Pfeifer G, Cjeka Z *et al.* A subcomplex of the proteasome regulatory particle required for ubiquitin-conjugate degradation and related to the COP9-signalosome and eIF3. *Cell* 1998; **94**: 615–623.
3. Lyapina S, Cope G, Shevchenko A, Serino G, Tsuge T, Zhou C *et al.* Promotion of NEDD-CUL1 conjugate cleavage by COP9 signalosome. *Science* 2001; **292**: 1382–1385.
4. He Q, Cheng P, Liu Y. The COP9 signalosome regulates the Neurospora circadian clock by controlling the stability of the SCFFWD-1 complex. *Genes Dev* 2005; **19**: 1518–1531.
5. Bornstein G, Ganoth D, Hershko A. Regulation of neddylation and deneddylation of cullin1 in SCFSkp2 ubiquitin ligase by F-box protein and substrate. *Proc Natl Acad Sci USA* 2006; **103**: 11515–11520.
6. Chew EH, Hagen T. Substrate-mediated regulation of cullin neddylation. *J Biol Chem* 2007; **282**: 17032–17040.
7. Wei N, Serino G, Deng XW. The COP9 signalosome: more than a protease. *Trends Biochem Sci* 2008; **33**: 592–600.
8. Menon S, Chi H, Zhang H, Deng XW, Flavell RA, Wei N. COP9 signalosome subunit 8 is essential for peripheral T cell homeostasis and antigen receptor-induced entry into the cell cycle from quiescence. *Nat Immunol* 2007; **8**: 1236–1245.

9. Panattoni M, Sanvito F, Basso V, Doglioni C, Casorati G, Montini E *et al.* Targeted inactivation of the COP9 signalosome impairs multiple stages of T cell development. *J Exp Med* 2008; **205**: 465–477.
10. Oren-Giladi P, Krieger O, Edgar BA, Chamovitz DA, Segal D. Cop9 signalosome subunit 8 (CSN8) is essential for Drosophila development. *Genes Cells* 2008; **13**: 221–231.
11. Serino G, Su H, Peng Z, Tsuge T, Wei N, Gu H *et al.* Characterization of the last subunit of the Arabidopsis COP9 signalosome: implications for the overall structure and origin of the complex. *Plant Cell* 2003; **15**: 719–731.
12. Yang X, Menon S, Lykke-Andersen K, Tsuge T, Di X, Wang X *et al.* The COP9 signalosome inhibits p27(kip1) degradation and impedes G1-S phase progression via deneddylation of SCF Cul1. *Curr Biol* 2002; **12**: 667–672.
13. Tomoda K, Kubota Y, Kato J. Degradation of the cyclin-dependent-kinase inhibitor p27Kip1 is instigated by Jab1. *Nature* 1999; **398**: 160–165.
14. Dohmann EM, Levesque MP, De Veylder L, Reichardt I, Jurgens G, Schmid M *et al.* The Arabidopsis COP9 signalosome is essential for G2 phase progression and genomic stability. *Development* 2008; **135**: 2013–2022.
15. Mundt KE, Porte J, Murray JM, Brikos C, Christensen PU, Caspari T *et al.* The COP9/ signalosome complex is conserved in fission yeast and has a role in S phase. *Curr Biol* 1999; **9**: 1427–1430.
16. Groisman R, Polanowska J, Kuraoka I, Sawada J, Saijo M, Drapkin R *et al.* The ubiquitin ligase activity in the DDB2 and CSA complexes is differentially regulated by the COP9 signalosome in response to DNA damage. *Cell* 2003; **113**: 357–367.
17. Harari-Steinberg O, Cantera R, Denti S, Bianchi E, Oron E, Segal D *et al.* COP9 signalosome subunit 5 (CSN5/Jab1) regulates the development of the Drosophila immune system: effects on Cactus, Dorsal and hematopoiesis. *Genes Cells* 2007; **12**: 183–195.
18. Su H, Huang W, Wang X. The COP9 signalosome negatively regulates proteasome proteolytic function and is essential to transcription. *Int J Biochem Cell Biol* 2009; **41**: 615–624.
19. Oron E, Tuller T, Li L, Rozovsky N, Yekutieli D, Rencus-Lazar S *et al.* Genomic analysis of COP9 signalosome function in Drosophila melanogaster reveals a role in temporal regulation of gene expression. *Mol Syst Biol* 2007; **3**: 108.
20. Chamovitz DA. Revisiting the COP9 signalosome as a transcriptional regulator. *EMBO Rep* 2009; **10**: 352–358.
21. Ullah Z, Buckley MS, Arnosti DN, Henry RW. Retinoblastoma protein regulation by the COP9 signalosome. *Mol Biol Cell* 2007; **18**: 1179–1186.
22. Tomoda K, Kubota Y, Arata Y, Mori S, Maeda M, Tanaka T *et al.* The cytoplasmic shuttling and subsequent degradation of p27Kip1 mediated by Jab1/CSN5 and the COP9 signalosome complex. *J Biol Chem* 2002; **277**: 2302–2310.
23. Sharon M, Mao H, Boeri Erba E, Stephens E, Zheng N, Robinson CV. Symmetrical modularity of the COP9 signalosome complex suggests its multifunctionality. *Structure* 2009; **17**: 31–40.
24. Lykke-Andersen K, Schaefer L, Menon S, Deng XW, Miller JB, Wei N. Disruption of the COP9 signalosome Csn2 subunit in mice causes deficient cell proliferation, accumulation of p53 and cyclin E, and early embryonic death. *Mol Cell Biol* 2003; **23**: 6790–6797.
25. Yan J, Walz K, Nakamura H, Carattini-Rivera S, Zhao Q, Vogel H *et al.* COP9 signalosome subunit 3 is essential for maintenance of cell proliferation in the mouse embryonic epiblast. *Mol Cell Biol* 2003; **23**: 6798–6808.
26. Tomoda K, Yoneda-Kato N, Fukumoto A, Yamanaka S, Kato JY. Multiple functions of Jab1 are required for early embryonic development and growth potential in mice. *J Biol Chem* 2004; **279**: 43013–43018.
27. Denti S, Fernandez-Sanchez ME, Rogge L, Bianchi E. The COP9 signalosome regulates Skp2 levels and proliferation of human cells. *J Biol Chem* 2006; **281**: 32188–32196.
28. Fausto N, Campbell JS, Riehle KJ. Liver regeneration. *Hepatology* 2006; **43** (2 Suppl 1): S45–S53.
29. Yeoh GC, Ernst M, Rose-John S, Akhurst B, Payne C, Long S *et al.* Opposing roles of gp130-mediated STAT-3 and ERK-1/ 2 signaling in liver progenitor cell migration and proliferation. *Hepatology* 2007; **45**: 486–494.
30. Postic C, Shiota M, Niswender KD, Jetton TL, Chen Y, Moates JM *et al.* Dual roles for glucokinase in glucose homeostasis as determined by liver and pancreatic beta cell-specific gene knock-outs using Cre recombinase. *J Biol Chem* 1999; **274**: 305–315.
31. Oertel M, Shafritz DA. Stem cells, cell transplantation and liver repopulation. *Biochim Biophys Acta* 2008; **1782**: 61–74.
32. Bird TG, Lorenzini S, Forbes SJ. Activation of stem cells in hepatic diseases. *Cell Tissue Res* 2008; **331**: 283–300.
33. Polager S, Ginsberg D. E2F – at the crossroads of life and death. *Trends Cell Biol* 2008; **18**: 528–535.
34. Van Hul NK, Abarca-Quinones J, Sempoux C, Horsmans Y, Leclercq IA. Relation between liver progenitor cell expansion and extracellular matrix deposition in a CDE-induced murine model of chronic liver injury. *Hepatology* 2009; **49**: 1625–1635.
35. Davies RA, Knight B, Tian YW, Yeoh GC, Olynyk JK. Hepatic oval cell response to the choline-deficient, ethionine supplemented model of murine liver injury is attenuated by the administration of a cyclo-oxygenase 2 inhibitor. *Carcinogenesis* 2006; **27**: 1607–1616.
36. Kisseleva T, Brenner DA. Fibrogenesis of parenchymal organs. *Proc Am Thorac Soc* 2008; **5**: 338–342.
37. Xu Z, Chen L, Leung L, Yen TS, Lee C, Chan JY. Liver-specific inactivation of the Nrf1 gene in adult mouse leads to nonalcoholic steatohepatitis and hepatic neoplasia. *Proc Natl Acad Sci USA* 2005; **102**: 4120–4125.
38. Kopanja D, Stoyanova T, Okur MN, Huang E, Bagchi S, Raychaudhuri P. Proliferation defects and genome instability in cells lacking Cul4A. *Oncogene* 2009; **28**: 2456–2465.